Co-detection of dopamine and glucose with high temporal resolution

catalysts

MDPI

Communication

Co-Detection of Dopamine and Glucose with High Temporal Resolution

Jenny Bergman [1], Lisa Mellander [2], Yuanmo Wang [3] and Ann-Sofie Cans [3,*]

[1] Department of Chemistry and Molecular Biology, Gothenburg University, 41296 Gothenburg, Sweden; jenny.bergman@chem.gu.se
[2] Department of Physiology, Institute of Neuroscience and Physiology, University of Gothenburg, 41390 Gothenburg, Sweden; lisa.mellander@gu.se
[3] Department of Chemistry and Chemical Engineering, Chalmers University of Technology, 41296 Gothenburg, Sweden; yuanmo@chalmers.se
* Correspondence: cans@chalmers.se; Tel.: +46-31-772-1000

Received: 6 December 2017; Accepted: 15 January 2018; Published: 19 January 2018

Abstract: Neuronal activity and brain glucose metabolism are tightly coupled, where triggered neurotransmission leads to a higher demand for glucose. To better understand the regulation of neuronal activity and its relation to high-speed metabolism, development of analytical tools that can temporally resolve the transients of vesicular neurotransmitter release and fluctuations of metabolites such as glucose in the local vicinity of the activated neurons is needed. Here we present an amperometric biosensor design for rapid co-detection of glucose and the neurotransmitter dopamine. The sensor is based on the immobilization of an ultra-thin layer of glucose oxidase on to a gold-nanoparticle-covered carbon fiber microelectrode. Our electrode, by altering the potential applied at the sensor surface, allows for the high-speed recording of both glucose and dopamine. We demonstrate that, even though glucose is electrochemically detected indirectly through the enzymatic product and the electroactive dopamine is sensed directly, when exposing the sensor surface to a mixture of the two analytes, fluctuations in glucose and dopamine concentrations can be visualized with similar speed and at a millisecond time scale. Hence, by minimizing the enzyme coating thickness at the sensor surface, dual detection of glucose and dopamine can be realized at the same sensor surface and at time scales necessary for monitoring fast metabolic alterations during neurotransmission.

Keywords: biosensor; glucose; glucose oxidase; amperometry; co-detection; temporal resolution; gold nanoparticles; microelectrode

1. Introduction

Enzymes are highly specific biocatalysts, converting a substrate to a product, making them excellent for incorporation in sensors aimed at selective detection of analytes that are otherwise difficult to detect. The first enzymatic biosensor was developed in the 1960s by Clark and Lyon for the detection of glucose with the use of the enzyme glucose oxidase (GOx) as part of the detection scheme [1]. Since then, there have been a tremendous number of biosensors developed for applications within the food industry, pharmacology, neurochemistry, environmental analysis, and chemistry [2–12]. The field of biosensors has been extensively expanded and a vast array of methods for detection has been explored [13–21]. Electrochemical detection has several advantages, such as fast sample rates, the possibility to miniaturize the sensor by the use of microelectrodes, and high biocompatibility of the electrode material where, e.g., carbon and gold have been successfully used for in vivo applications [22–24]. In addition to its use in biosensor design, electrochemical detection is also frequently employed in the study of electroactive substances, where the analyte undergoes a redox

reaction directly at the electrode surface when a redox potential is applied. The neurotransmitter dopamine is extensively explored by electrochemistry due to its ability to easily oxidize at a positively polarized electrode [25,26]. Dopamine is related to the reward system of the brain, and it has a central role in Parkinson's disease [27,28] as well as in addiction [29]. Glucose is the primary source of energy in the mammalian brain as its metabolism generates ATP, the fuel for cellular maintenance and neurotransmission. It has been shown that an increase in local neuronal activity is associated with a higher glucose concentration in the activated brain area and that glucose-excited neurons sense fluctuations in local glucose levels [30,31]. Therefore, the ability to co-detect rapid local fluctuations of dopamine and glucose has the potential to reveal new insights in how neuronal activity is connected to and regulated by the energy metabolism in the brain [32].

The construction of enzyme-based electrochemical biosensors relies on the immobilization of enzymes at an electrode surface where the enzymatic activity product can be detected [33,34]. Enzymes adsorbing to a flat surface have a tendency to flatten out, which causes an alteration of their protein tertiary structure and often thereby a reduction in enzymatic activity. In order to prevent enzyme denaturation upon adsorption to an electrode surface, several methods for enzyme immobilization have been developed, e.g., enzyme attachment using cross-linkers, enzyme entrapment in polymers, and the incorporation of nanomaterials at the sensor surface as support for enzymes to bind [35–41]. Several studies have shown that immobilizing enzymes on a high curvature surface is beneficial for retaining enzymatic activity by minimizing changes in the tertiary structure of the enzyme [42–45]. Modifying the electrode surface with nanomaterials such as nanotubes and nanoparticles (NPs) introduces a high curvature support for enzyme immobilization. Additionally, the introduction of nanostructures will also increase the electrode surface area, thereby allowing for a higher enzyme loading that increases the sensitivity of the sensor. Gold nanomaterials, such as gold nanoparticles (AuNPs), have been widely used due to their high biocompatibility and increased ability to oxidize/reduce enzymatic electroactive products, e.g., hydrogen peroxide (H_2O_2) [46–49].

Earlier reported glucose biosensors have not focused on applications that demand high temporal resolution. Our aim is to develop novel miniaturized electrochemical biosensors that can be used for analyzing real-time rapid fluctuations of non-electroactive molecules at single secretory cells and locally by groups of cells in brain tissue. We have previously shown that a two-sequential enzyme system, acetylcholine esterase (AChE) and choline oxidase (ChO), immobilized as a monolayer on to an AuNP-coated carbon fiber microelectrode (CFME) can be used to detect the vesicular release of the non-electroactive neurotransmitter acetylcholine with a millisecond temporal resolution [50]. Here, we immobilize a single enzyme system (GOx) to the surface of AuNPs covering a CFME and we investigate the temporal resolution for glucose detection and compare it with that of the electroactive neurotransmitter dopamine. Glucose, a non-electroactive molecule, must undergo an enzymatic catalytic reaction by the immobilized GOx at the electrode surface in order to generate an electroactive product that can be detected by the electrode. Each glucose molecule is enzymatically converted to gluconic acid and H_2O_2, which is then reduced at the AuNP surface of the electrode held at a potential of −0.5 V (vs. Ag/AgCl), where one H_2O_2 molecule generates two electrons according to the following chemical reactions:

$$\text{glucose} + \ O_2 \ \rightarrow \text{gluconic acid} \ + H_2O_2$$

$$H_2O_2 + \ 2H^+ + 2e^- \ \rightarrow \ 2\,H_2O$$

In the sensor schemes used here for the high temporal dual detection of glucose and dopamine, dopamine is oxidized at +0.5 V (vs. Ag/AgCl), a potential sufficient for diffusion limited dopamine oxidation, and a potential where H_2O_2 not is detectable (Figure S1). In order to compare the kinetics for the detection of glucose and dopamine, the two analytes must be selectively detected at the same sensor. Here we monitor the kinetics and selective detection of glucose undergoing a catalytic reaction by the immobilized GOx, resulting in the production of H_2O_2, which diffuses to the electrode surface for electrochemical detection, and compare it to the speed for the detection of dopamine, which,

following diffusion through the thin coating of immobilized enzyme, is directly detected when it is in contact with the electrode surface. The results demonstrate the uniqueness of this sensor, as it allows for the dual detection of a non-electroactive analyte and an electroactive one with the same time resolution.

2. Results and Discussion

2.1. Preparation of the Biosensor

AuNPs were electrodeposited to the electrode surface by placement in a 0.5 mM $HAuCl_4$ solution and subsequent reduction of Au^{3+} to Au^0 through application of a large overpotential (−0.6 V vs. Ag/AgCl) for 24 s, a method originally developed by Finot et al. [51]. The electrodeposition parameters have previously been optimized by our lab for a CFME 33 µm in diameter and provide a coating of AuNPs approximately 20 nm in diameter with a 30% electrode surface coverage [50]. Monolayer enzyme coverage at the surface of nanoparticles has been demonstrated to be beneficial in several aspects, e.g., a greater accessibility of the enzyme active site, a reduction of steric hindrance between enzymes, and a faster diffusion of the enzymatic product to the electrode surface [42–44]. Glucose oxidase is an enzyme unwilling to form multiple layers when it is immobilized upon a surface [52]. We have previously developed a method for quantifying the number of GOx enzymes immobilized onto the surface of AuNPs coating a glassy carbon electrode, resulting in close to a monolayer coverage at an AuNP surface [53]. Based on these previous results, we estimate that the conditions used here for GOx immobilization (2 mg mL^{-1} and an incubation time of 2 h at room temperature) results in approximately monolayer coverage of GOx.

2.2. Biosensor Characterization

The modification of the carbon surface with AuNPs fills two functions in this sensor design. It provides a high curvature surface for enzyme immobilization and provides an electrode surface with an enhanced ability to detect the enzymatic product H_2O_2. The enhanced detection ability is important as H_2O_2 can only be reduced at the Au surface of the electrode—not at the carbon—and at the potential applied in these experiments. As a consequence, since the total deposited Au surface varies between electrodes, all current responses should be normalized to the total AuNP surface area of each electrode in order to compare the response magnitude between electrodes. The AuNP–CFME response to H_2O_2 shows linearity over a large concentration range (10 µM–10 mM) where the response in the lower concentration range (10 µM–1 mM) is shown in Figure 1b. The sensitivity to H_2O_2 at the AuNP–CFME was determined to be 8.4 ± 0.5 pA mM^{-1} μm^{-2} (R-square 0.992) in the linear range of H_2O_2 concentrations tested (Figure S2). The enzymatic sensor was exposed to glucose concentrations between 10 µM and 10 mM (Figure S3) to generate a Michaelis–Menten curve revealing a K_M for the biosensor of 0.07 ± 0.03 mM. Typically, enzymes in solution have K_M values ranging between 10^{-1} M (low affinity) and 10^{-7} M (high affinity) [54]. At lower concentrations of glucose, the sensor demonstrates a linear response between 10 µM and 100 µM, while the current reached a plateau at 1 mM glucose (Figure 1a). The sensitivity of glucose within the linear range was determined to be 1.9 ± 0.04 pA mM^{-1} μm^{-2} (R-square 0.999), which is approximately one quarter the sensitivity of the response towards H_2O_2 by the AuNP–CFME, indicating a highly retained enzymatic activity of the GOx enzyme when immobilized to the sensor surface in this concentration range. The limit of detection for this biosensor was determined to 10 µM (3σ).

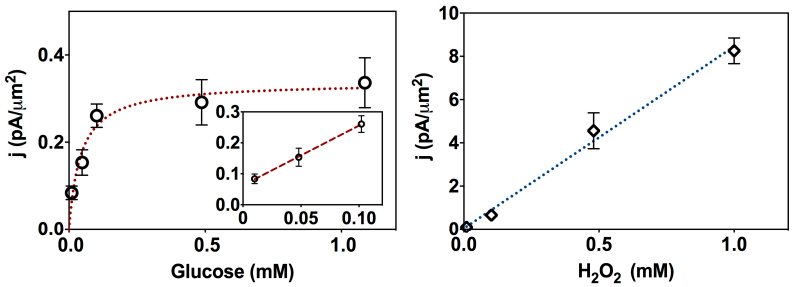

(**a**) (**b**)

Figure 1. (**a**) A reproducible calibration curve for glucose using the glucose oxidase and gold nanoparticle modified carbon fiber microelectrode (GOx–AuNP–CFME) (n = 7–10) when recording the cathodic current at −0.5 V (vs. an Ag/AgCl reference electrode) and normalized the current response by the total AuNP surface area at each electrode. Inset: the linear detection range of glucose from 10 to 100 μM. (**b**) The linear response towards H_2O_2 by AuNP–CFME (n = 3–6) at the lower concentration range tested and recording the cathodic current at −0.5 V (vs. an Ag/AgCl reference electrode). All errors are shown as standard error of the mean.

Since GOx is an extensively used enzyme in biosensor fabrication with many different approaches for biosensor design, reported values for K_M, sensitivity, linear range, and limit of detection for GOx-based sensors are very heterogeneous, as reviewed by Zaidi and Shin [55], with K_M values ranging between 15 μM and 2 mM, while the sensitivity varies between 10 and 5000 μA mM^{-1} cm^{-2} and the limit of detection between 0.07 μM and 4.8 mM. Hence, the values obtained for our sensor fits well in the range of what has been previously determined for nanostructured glucose sensors.

The specificity of the biosensor for glucose is of importance for possible future in vivo applications for monitoring, e.g., alterations in glucose metabolism in relation to local neuronal activity. To evaluate possible common interferences for the sensor in brain tissue, several biologically relevant substances were tested; the electroactive neurotransmitters dopamine and serotonin, the non-electroactive neurotransmitters glutamate and acetylcholine, and two other commonly interfering molecules, ascorbic acid and lactate. Except for lactate which is present at concentrations of approximately 1 mM, these molecules generally occur in low concentrations in the brain tissue environment, typically in the μM range [56–59], while the average resting concentration of glucose in the human brain during normoglycemia is around 1 mM [60]. As seen in Figure 2, at 1 mM, none of the tested possible interferences gave a response greater than 25% of the glucose signal, indicating that interfering species will not be a limitation for glucose detection during in vivo measurements in the brain.

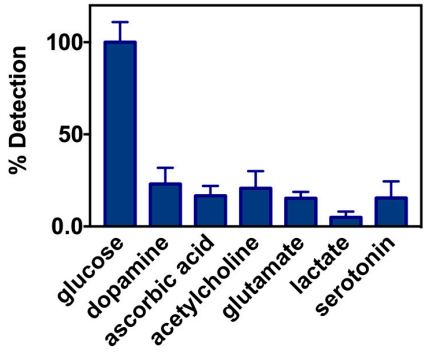

Figure 2. The resulting cathodic current recorded at −0.5 V and illustrating selectivity by the glucose oxidase and gold nanoparticle modified carbon fiber microelectrode (GOx–AuNP–CFME) (n = 3–6) after exposure to different possible interfering analytes in the extracellular brain tissue environment with concentrations of 1 mM and in the presence of 1 mM glucose. Due to the possibility of analyte detection also by the carbon at the electrode surface, the signal is not normalized to total Au surface area. All errors are shown as standard error of the mean.

To investigate and compare the response time for the sensor to fast local alterations in glucose and dopamine concentrations, the kinetics of the sensor was tested by exposing the sensor surface to controlled rapid fluctuations of the two analytes in solution. As schematically displayed in Figure 3, by placing the tip of a glass micropipette filled with 25 mM glucose and 20 μM dopamine solution at approximately 30 μm distance from the sensor surface, 500 ms microinjection puffs were applied toward the electrode surface using a microinjector. Due to the higher sensor sensitivity for dopamine compared to glucose, the analyte concentrations were adjusted to result in similar peak currents.

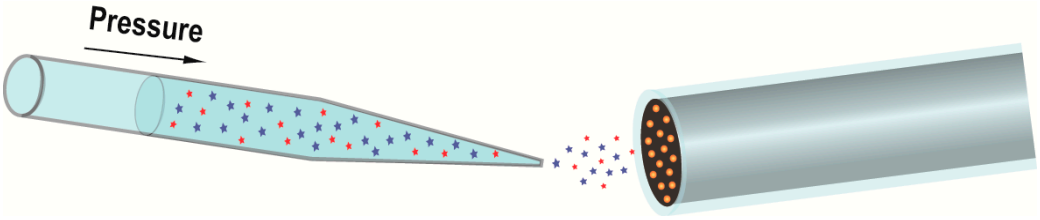

Figure 3. A schematic of the experimental set-up for comparing the kinetic response for detection of glucose (red stars) and dopamine (blue stars) using the glucose oxidase and gold nanoparticle modified carbon fiber microelectrode (GOx–AuNP–CFME). Here a micropipette filled with a solution mixture containing dopamine (20 μM) and glucose (25 mM) is placed approximately 30 μm from the surface of a GOx–AuNP–CFME. Using a microinjector pump, 500 ms puffs of the solution mixture is injected against the sensor surface placed in buffer solution creating a controlled rapid fluctuation of the two analytes towards the electrode. By applying a potential of +0.5 V and −0.5 V to the sensor surface (vs. an Ag/AgCl reference electrode) the dopamine and glucose are amperometrically detected, through a reduction or oxidation reaction, respectively.

When the electrode was held at −0.5 V, a sharp rise in reductive current was observed as the puff of analyte solution reached the sensor surface, followed by a current decline to baseline as the pressure on the micropipette was switched off (Figure 4). The response to dopamine was tested by puffing the dopamine and glucose containing solution towards the same electrode, while instead applying a potential of +0.5 V to the electrode surface. The electrode response to dopamine was used for evaluation of the ability of the sensor to co-detect glucose and dopamine, as well as to compare the kinetic response for the two analytes. The results show that, in the initial rise of the current peak, the enzymatically catalyzed reaction of glucose to H_2O_2, followed by the reduction of H_2O_2 at the electrode, is as fast as the direct oxidation of the electroactive dopamine, with rise times (25–75%) of the peaks of 300 ms for dopamine and 260 ms for glucose. However, the current transient returns to the baseline faster for glucose than for dopamine. A possible explanation for this observation could be the higher sensor detection limit for glucose as compared to dopamine, since the concentration of analyte will quickly decrease as the pressure from the microinjector is switched off, and glucose will more rapidly reach a concentration that is not detected by the electrode.

In summary, the results from these experiments demonstrate that, by altering the potential applied to the sensor surface according to the respective redox potential for glucose-derived H_2O_2 and dopamine, rapid fluctuations of these analytes can be monitored. Even though the sensitivity for detection of glucose versus dopamine at this sensor scheme is significantly reduced, by limiting the coating to an ultra-thin enzyme layer during fabrication, the temporal resolution of glucose concentration fluctuation recordings in solution is comparable to the speed of that for dopamine. Hence, this sensor design provides a tool for correlating dopamine activity with metabolic glucose levels at a time scale relevant for neuronal communication. As development of many enzyme-coated electrochemical biosensors are functionalized with nanomaterials, this methodology can also be applied for construction of biosensors that aim for dual detection of other fast fluctuating non-electroactive and electroactive analytes that are involved in neuronal communication.

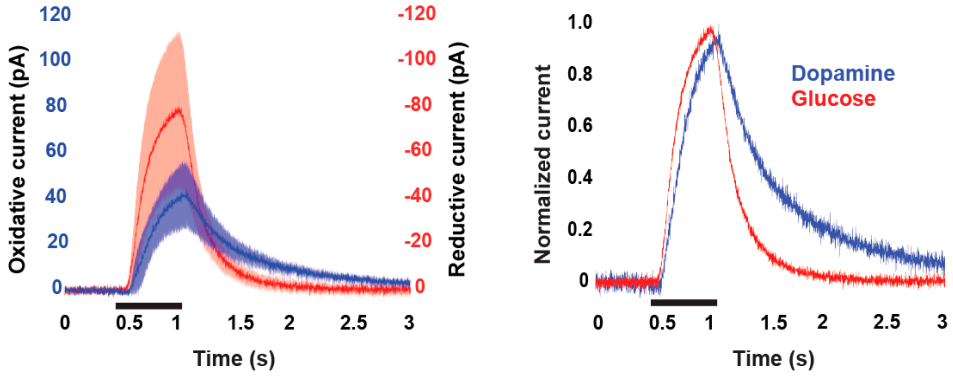

Figure 4. (**a**) The temporal response for detection of puffing a solution containing 20 µM dopamine (blue) and 25 mM glucose (red) against the biosensor surface when applying a potential of +0.5 V and −0.5 V vs. an Ag/AgCl reference electrode, respectively. (**b**) Normalized detection response of the dopamine- and glucose-containing solution. The black band indicates the timing for the 500 ms injection pulse applied to the glass microinjection pipette.

3. Materials and Methods

3.1. Chemical Reagents

Glucose oxidase (type VII) from *Aspergillus niger*, phosphate-buffered saline tablets (10 mM, pH 7.2), sulfuric acid, copper sulfate, tetrachloroaurate, serotonin chloride, dopamine chloride, glucose, lactic acid, monosodium glutamate, acetylcholine chloride, ascorbic acid, ferrocene methanol, tungsten wire, and hydrogen peroxide were purchased from Sigma-Aldrich (St. Louis, MO, USA). All reagents used where of reagent grade and used as received. Deionized water (resistivity $\geq$ 18 MΩ cm) was used in all experiments.

3.2. Electrochemical Set-Up

Electrochemical measurements, cyclic voltammetry, chronoamperometry, and amperometry were performed using a two-electrode system with a computer-controlled 1000C Series Multi-Potentiostat (CH Instruments, Austin, TX, USA) or an Axopatch potentiostat 200B (Axon Instruments, Foster City, CA, USA). For all experiments, a saturated Ag/AgCl was used as a reference electrode and all potentials are reported against this reference electrode unless otherwise stated.

3.3. Preparation of a 33 µm CFME

Carbon fiber microelectrodes were prepared by aspirating single 33-µm diameter carbon fibers (Cytec Engineered Materials, Tempe, AZ, USA) into borosilicate glass capillaries (1.2 mm O.D., 0.69 mm I.D., Sutter Instrument Co., Novato, CA, USA). The filled capillaries were then pulled to a taper using a commercial micropipette puller (P-1000; Sutter Instrument Co., Novato, CA, USA) and epoxy (Epoxy Technology, Billerica, MA, USA) was used to seal the glass-carbon fiber junction of the electrode. The electrode tips were cut using a scalpel and polished at a 45° angle on a diamond dust-embedded micropipette beveling wheel (Narishige, Inc., London, UK). The electrodes were backfilled with silver paint or KCl (3 M) and a metal wire (tungsten and silver, respectively) was inserted and used as the connection to the potentiostat. All electrodes were tested in 1 mM ferrocene methanol by performing cyclic voltammetry between −0.2 and +0.6 V at 0.1 V s^{-1} in order to make sure the electrodes where well-functioning by evaluating their voltammograms prior to each experiment.

3.4. Functionalization with AuNP

Electrodes were functionalized with AuNP by an electrochemical deposition similar to Finot et al. [51] with minor alterations. The CFME and an Ag/AgCl reference electrode were immersed in a 0.5 mM solution of $HAuCl_4$ in 0.5 M H_2SO_4. A potential of +1.2 V was applied for 10 s followed by a potential of −0.6 V for 24 s. The AuNP surface area was then measured electrochemically by performing a linear sweep from +1.4 V (potential held for 5 s) to +0.5 V at a rate of 0.1 V s^{-1} in 0.5 M H_2SO_4. Here a $Cu/CuSO_4$ reference electrode was used to avoid chloride contamination. The resulting peak at approximately +0.8 V was integrated by the inbuilt software in the 1000C Series Multi-Potentiostat (CH Instruments, Austin, TX, USA) and the obtained charge was divided with a factor of 4.89 pC μm^{-2} as used by Finot et al. [51]. The electrodes used for further experiments had a total gold surface area of approximately 2000 μm^2.

3.5. Immobilization of Enzymes

The tip of each electrode was immersed in a solution containing 2 mg mL^{-1}. Glucose oxidase in phosphate-buffered saline, (10 mM, pH 7.2) for 2 h at room temperature. After immersion, the tip of each electrode was washed with deionized water and stored in a solution of phosphate-buffered saline (PBS) (10 mM, pH 7.2) at 4 °C when not used immediately for experiments.

3.6. Characterization of the Glucose Sensor

The detection of glucose was tested using chronoamperometry in PBS. Briefly, a constant potential where no reaction occurs (at 0 V) was held for a certain time (10 s) and then immediately changed to −0.5 V where the reduction of the enzymatic product hydrogen peroxide takes place and held constant until the resulting reduction current had reached a steady state (30 s). A glucose calibration curve was performed from 10 µM to 10 mM using freshly prepared solutions from a 1 M glucose stock solution by adding aliquots of 1, 10, and 100 mM to the bulk PBS solution followed by convection induced by a pipette. The response of the following interferences, acetylcholine, lactate, dopamine, serotonin, ascorbic acid, and glutamate were tested in a 1 mM concentration in the presence of 1 mM glucose with the same chronoamperometry method as described above. The AuNP-modified CFME response to the enzymatic product hydrogen peroxide was performed using the same method and concentrations as for the glucose calibration. Statistical analysis and enzyme kinetic parameters where analyzed using GraphPad Prism 7 (La Jolla, CA, USA).

For the kinetic characterization, a micropipette (o.d. 1 mm, i.d. 0.78 mm, with filament; Harvard Apparatus, Holliston, MA, USA) was pulled on a commercial filament puller (P-1000; Sutter Instrument Co., Novato, CA, USA) and back-filled with a solution containing 20 µM dopamine and 25 mM glucose in PBS. The pipette was placed together with a glucose sensor in a dish containing PBS on an Olympus IX-71 microscope (Olympus, Melville, NY, USA). Hydraulic micromanipulators (MHW-3, Narishige, Tokyo, Japan) were used to position the pipette approximately 30 µm away from the electrode surface. A potential was applied at the electrode vs. a silver/silver chloride reference electrode (World Precision Instruments, Inc., Sarasota, FL, USA) also placed in the dish. A commercial patch-clamp instrument (Axopatch 200B; Axon Instruments, Foster City, CA, USA) was used to control the potential at the working electrode, +0.5 V for the detection of dopamine, while a negative potential of −0.5 V was applied to detect the enzymatic product hydrogen peroxide. Pressure was applied to the back of the pipette (Picospritzer II; General Valve Instruments, Fairfield, NJ, USA) to create a 500 ms puff of solution towards the electrode, resulting in a peak in either reductive or oxidative current depending on the applied potential. The current, digitized at 5 kHz, was displayed in real time (AxoScope 8.1; Axon Instruments, Union City, CA, USA) and stored digitally. The peaks were analyzed in Igor Pro 6 (Version 6.2.2.0; WaveMetrics, Lake Oswego, OR, USA) using an Igor Procedure File designed for analysis of quantal release by the group of David Sulzer [61].

Supplementary Materials: The following are available online at www.mdpi.com/2073-4344/8/1/34/s1, Figure S1: Cyclic voltammetry of a CFME–AuNP in PBS buffer (black) 5 mM H_2O_2 (red) and 10 mM H_2O_2. The voltammogram

shows that H_2O_2 is reduced at potentials below −0.25 V and that no oxidation reaction occurs involving H_2O_2 when potential +0.5 V is applied. Figure S2: The AuNP–CFME response to H_2O_2 shows linearity over a large concentration range (10 μM–10 mM) and display a sensitivity of 8.4 ± 0.5 pA mM^{-1} μm^{-2}. Figure S3: The GOx–AuNP–CFME response to glucose for the whole concentration range tested (10 μM–10 mM).

Acknowledgments: The authors acknowledge the Swedish Research Council for funding.

Author Contributions: J.B., Y.W., and A.-S.C. conceived the project. J.B. designed and performed the experiments for characterization of the sensor, and Y.W. took part in the early development stage for the sensor characterization. J.B. performed the sensor characterization experiments and analyzed the data; J.B. and L.M. designed and performed the experiments for temporal characterization of the sensor, and L.M. analyzed the data. J.B. wrote the paper together with L.M. and A.-S.C.

Conflicts of Interest: The authors declare no conflict of interest. The founding sponsors had no role in the design of the study; in the collection, analyses, or interpretation of data; in the writing of the manuscript; or in the decision to publish the results.

References

1. Clark, L.C.; Lyons, C. Electrode Systems for Continous Monitoring in cardiovascular surgery cardivascular surgery. *Ann. N. Y. Acad. Sci.* **1962**, *102*, 29–45. [CrossRef] [PubMed]
2. Khan, M.S.; Misra, S.K.; Schwartz-Duval, A.S.; Daza, E.; Ostadhossein, F.; Bowman, M.; Jain, A.; Taylor, G.; McDonagh, D.; Labriola, L.T.; et al. Real-Time Monitoring of Post-Surgical and Post-Traumatic Eye Injuries Using Multilayered Electrical Biosensor Chip. *ACS Appl. Mater. Interfaces* **2017**, *9*, 8609–8622. [CrossRef] [PubMed]
3. Monosik, R.; Stredansky, M.; Tkac, J.; Sturdik, E. Application of Enzyme Biosensors in Analysis of Food and Beverages. *Food Anal. Methods* **2012**, *5*, 40–53. [CrossRef]
4. Prodromidis, M.I.; Karayannis, M.I. Enzyme based amperometric biosensors for food analysis. *Electroanalysis* **2002**, *14*, 241–261. [CrossRef]
5. Rocchitta, G.; Spanu, A.; Babudieri, S.; Latte, G.; Madeddu, G.; Galleri, G.; Nuvoli, S.; Bagella, P.; Demartis, M.I.; Fiore, V.; et al. Enzyme Biosensors for Biomedical Applications: Strategies for Safeguarding Analytical Performances in Biological Fluids. *Sensors* **2016**, *16*, 780. [CrossRef] [PubMed]
6. Verma, N.; Bhardwaj, A. Biosensor Technology for Pesticides—A review. *Appl. Biochem. Biotechnol.* **2015**, *175*, 3093–3119. [CrossRef] [PubMed]
7. Dale, N.; Hatz, S.; Tian, F.; Llaudet, E. Listening to the brain: Microelectrode biosensors for neurochemicals. *Trends Biotechnol.* **2005**, *23*, 420–428. [CrossRef] [PubMed]
8. Cordeiro, C.; de Vries, M.G.; Ngabi, W.; Oomen, P.E.; Cremers, T.I.F.H.; Westerink, B.H.C. In vivo continuous and simultaneous monitoring of brain energy substrates with a multiplex amperometric enzyme-based biosensor device. *Biosens. Bioelectron.* **2015**, *67*, 677–686. [CrossRef] [PubMed]
9. Kiyatkin, E.A.; Wakabayashi, K.T. Parsing glucose entry into the brain: Novel findings obtained with enzyme-based glucose biosensors. *ACS Chem. Neurosci.* **2014**, *6*, 108–116. [CrossRef] [PubMed]
10. Lourenço, C.F.; Ledo, A.; Laranjinha, J.; Gerhardt, G.A.; Barbosa, R.M. Microelectrode array biosensor for high-resolution measurements of extracellular glucose in the brain. *Sens. Actuators B Chem.* **2016**, *237*, 298–307. [CrossRef]
11. Santos, R.M.; Laranjinha, J.; Barbosa, R.M.; Sirota, A. Simultaneous measurement of cholinergic tone and neuronal network dynamics in vivo in the rat brain using a novel choline oxidase based electrochemical biosensor. *Biosens. Bioelectron.* **2015**, *69*, 83–94. [CrossRef] [PubMed]
12. Du, Y.; Zhang, W.; Wang, M. Sensing of Salivary Glucose Using Nano-Structured Biosensors. *Biosensors* **2016**, *6*, 10. [CrossRef] [PubMed]
13. Rauf, S.; Hayat Nawaz, M.A.; Badea, M.; Marty, J.L.; Hayat, A. Nano-engineered biomimetic optical sensors for glucose monitoring in diabetes. *Sensors* **2016**, *16*, 1931. [CrossRef] [PubMed]
14. Chen, C.; Xie, Q.; Yang, D.; Xiao, H.; Fu, Y.; Tan, Y.; Yao, S. Recent advances in electrochemical glucose biosensors: A review. *RSC Adv.* **2013**, *3*, 4473–4491. [CrossRef]
15. Devadoss, A.; Sudhagar, P.; Terashima, C.; Nakata, K.; Fujishima, A. Photoelectrochemical biosensors: New insights into promising photoelectrodes and signal amplification strategies. *J. Photochem. Photobiol. C* **2015**, *24*, 43–63. [CrossRef]

16. Papa, H.; Gaillard, M.; Gonzalez, L.; Chatterjee, J. Fabrication of Functionalized Carbon Nanotube Buckypaper Electrodes for Application in Glucose Biosensors. *Biosensors* **2014**, *4*, 449–460. [CrossRef] [PubMed]
17. Kitte, S.A.; Gao, W.; Zholudov, Y.T.; Qi, L.; Nsabimana, A.; Liu, Z.; Xu, G. Stainless Steel Electrode for Sensitive Luminol Electrochemiluminescent Detection of H_2O_2, Glucose, and Glucose Oxidase Activity. *Anal. Chem.* **2017**, *89*, 9864–9869. [CrossRef] [PubMed]
18. Theuer, L.; Lehmann, M.; Junne, S.; Neubauer, P.; Birkholz, M. Micro-Electromechanical Affinity Sensor for the Monitoring of Glucose in Bioprocess Media. *Int. J. Mol. Sci.* **2017**, *18*, 1235. [CrossRef] [PubMed]
19. He, Y.; Zheng, J.; Wang, B.; Ren, H. Double Biocatalysis Signal Amplification Glucose Biosensor Based on Porous Graphene. *Materials* **2017**, *10*, 1139. [CrossRef] [PubMed]
20. Li, C.; Chen, X.; Zhang, F.; He, X.; Fang, G.; Liu, J.; Wang, S. Design of Cyclic Peptide Based Glucose Receptors and Their Application in Glucose Sensing. *Anal. Chem.* **2017**, *89*, 10431–10438. [CrossRef] [PubMed]
21. Bornhoeft, L.; Biswas, A.; McShane, M. Composite Hydrogels with Engineered Microdomains for Optical Glucose Sensing at Low Oxygen Conditions. *Biosensors* **2017**, *7*, 8. [CrossRef] [PubMed]
22. Weltin, A.; Kieninger, J.; Urban, G.A. Microfabricated, amperometric, enzyme-based biosensors for in vivo applications. *Anal. Bioanal. Chem.* **2016**, *408*, 4503–4521. [CrossRef] [PubMed]
23. Xiao, T.; Wu, F.; Hao, J.; Zhang, M.; Yu, P.; Mao, L. In Vivo Analysis with Electrochemical Sensors and Biosensors. *Anal. Chem.* **2017**, *89*, 300–313. [CrossRef] [PubMed]
24. Bucher, E.S.; Wightman, R.M. Electrochemical Analysis of Neurotransmitters. *Annu. Rev. Anal. Chem.* **2015**, *8*, 239–261. [CrossRef] [PubMed]
25. Ferapontova, E.E. Electrochemical Analysis of Dopamine: Perspectives of Specific In Vivo Detection. *Electrochim. Acta* **2017**. [CrossRef]
26. Fox, M.E.; Wightman, R.M. Contrasting Regulation of Catecholamine Neurotransmission in the Behaving Brain: Pharmacological Insights from an Electrochemical Perspective. *Pharmacol. Rev.* **2017**, *69*, 12–32. [CrossRef] [PubMed]
27. Davie, C.A. A review of Parkinson's disease. *Br. Med. Bull.* **2008**, *86*, 109–127. [CrossRef] [PubMed]
28. Kalia, L.V.; Lang, A.E. Parkinson's disease. *Lancet* **2015**, *386*, 896–912. [CrossRef]
29. Nutt, D.J.; Lingford-Hughes, A.; Erritzoe, D.; Stokes, P.R. The dopamine theory of addiction: 40 years of highs and lows. *Nat. Rev. Neurosci.* **2015**, *16*, 305–312. [CrossRef] [PubMed]
30. Mergenthaler, P.; Lindauer, U.; Dienel, G.A.; Meisel, A. Sugar for the brain: The role of glucose in physiological and pathological brain function. *Trends Neurosci.* **2013**, *36*, 587–597. [CrossRef] [PubMed]
31. Zheng, H.; Wang, R.; Qu, J. Effect of different glucose supply conditions on neuronal energy metabolism. *Cogn. Neurodyn.* **2016**, *10*, 563–571. [CrossRef] [PubMed]
32. Smith, S.K.; Lee, C.A.; Dausch, M.E.; Horman, B.M.; Patisaul, H.B.; McCarty, G.S.; Sombers, L.A. Simultaneous Voltammetric Measurements of Glucose and Dopamine Demonstrate the Coupling of Glucose Availability with Increased Metabolic Demand in the Rat Striatum. *ACS Chem. Neurosci.* **2017**, *8*, 272–280. [CrossRef] [PubMed]
33. Grieshaber, D.; MacKenzie, R.; Voeroes, J.; Reimhult, E. Electrochemical Biosensors—Sensor Principles and Architectures. *Sensors* **2008**, *8*, 1400–1458. [CrossRef] [PubMed]
34. Kimmel, D.W.; LeBlanc, G.; Meschievitz, M.E.; Cliffel, D.E. Electrochemical sensors and biosensors. *Anal. Chem.* **2012**, *84*, 685–707. [CrossRef] [PubMed]
35. Bhardwaj, T. A Review on Immobilization Techniques of Biosensors. *Int. J. Eng. Res. Technol.* **2014**, *3*, 294–298.
36. Cosnier, S. Biosensors based on electropolymerized films: New trends. *Anal. Bioanal. Chem.* **2003**, *377*, 507–520. [CrossRef] [PubMed]
37. Homaei, A.A.; Sariri, R.; Vianello, F.; Stevanato, R. Enzyme immobilization: An update. *J. Chem. Biol.* **2013**, *6*, 185–205. [CrossRef] [PubMed]
38. Jesionowski, T.; Zdarta, J.; Krajewska, B. Enzyme immobilization by adsorption: A review. *Adsorption* **2014**, *20*, 801–821. [CrossRef]
39. Noll, T.; Noll, G. Strategies for "wiring" redox-active proteins to electrodes and applications in biosensors, biofuel cells, and nanotechnology. *Chem. Soc. Rev.* **2011**, *40*, 3564–3576. [CrossRef] [PubMed]
40. Putzbach, W.; Ronkainen, N.J. Immobilization Techniques in the Fabrication of Nanomaterial-Based Electrochemical Biosensors: A Review. *Sensors* **2013**, *13*, 4811–4840. [CrossRef] [PubMed]

41. Vasylieva, N.; Maucler, C.; Meiller, A.; Viscogliosi, H.; Lieutaud, T.; Barbier, D.; Marinesco, S. Immobilization method to preserve enzyme specificity in biosensors: Consequences for brain glutamate detection. *Anal. Chem.* **2013**, *85*, 2507–2515. [CrossRef] [PubMed]
42. Asuri, P.; Karajanagi, S.S.; Vertegel, A.A.; Dordick, J.S.; Kane, R.S. Enhanced stability of enzymes adsorbed onto nanoparticles. *J. Nanosci. Nanotechnol.* **2007**, *7*, 1675–1678. [CrossRef] [PubMed]
43. Cans, A.-S.; Dean, S.L.; Reyes, F.E.; Keating, C.D. Synthesis and characterization of enzyme-Au bioconjugates: HRP and fluorescein-labeled HRP. *Nanobiotechnology* **2007**, *3*, 12–22. [CrossRef]
44. Gagner, J.E.; Lopez, M.D.; Dordick, J.S.; Siegel, R.W. Effect of gold nanoparticle morphology on adsorbed protein structure and function. *Biomaterials* **2011**, *32*, 7241–7252. [CrossRef] [PubMed]
45. Keighron, J.D.; Åkesson, S.; Cans, A.-S. Coimmobilization of acetylcholinesterase and choline oxidase on gold nanoparticles: Stoichiometry, activity, and reaction efficiency. *Langmuir* **2014**, *30*, 11348–11355. [CrossRef] [PubMed]
46. Li, Y.; Schluesener, H.J.; Xu, S. Gold nanoparticle-based biosensors. *Gold Bull.* **2010**, *43*, 29–41. [CrossRef]
47. Luo, X.-L.; Xu, J.J.; Du, Y.; Chen, H.Y. A glucose biosensor based on chitosan–glucose oxidase–gold nanoparticles biocomposite formed by one-step electrodeposition. *Anal. Biochem.* **2004**, *334*, 284–289. [CrossRef] [PubMed]
48. Zhang, S.; Wang, N.; Niu, Y.; Sun, C. Immobilization of glucose oxidase on gold nanoparticles modified Au electrode for the construction of biosensor. *Sens. Actuator B Chem.* **2005**, *109*, 367–374. [CrossRef]
49. Zhao, S.; Zhang, K.; Bai, Y.; Yang, W.; Sun, C. Glucose oxidase/colloidal gold nanoparticles immobilized in Nafion film on glassy carbon electrode: Direct electron transfer and electrocatalysis. *Bioelectrochemistry* **2006**, *69*, 158–163. [CrossRef] [PubMed]
50. Keighron, J.D.; Wigström, J.; Kurczy, M.E.; Bergman, J.; Wang, Y.; Cans, A.S. Amperometric detection of single vesicle acetylcholine release events from an artificial cell. *ACS Chem. Neurosci.* **2015**, *6*, 181–188. [CrossRef] [PubMed]
51. Finot, M.O.; Braybrook, G.D.; McDermott, M.T. Characterization of electrochemically deposited gold nanocrystals on glassy carbon electrodes. *J. Electroanal. Chem.* **1999**, *466*, 234–241. [CrossRef]
52. Ferreyra, N.; Coche-Guérente, L.; Labbé, P. Construction of layer-by-layer self-assemblies of glucose oxidase and cationic polyelectrolyte onto glassy carbon electrodes and electrochemical study of the redox-mediated enzymatic activity. *Electrochim. Acta* **2004**, *49*, 477–484. [CrossRef]
53. Bergman, J.; Wang, Y.; Wigström, J.; Cans, A.S. Counting the number of enzymes immobilized onto a nanoparticle-coated electrode. *Anal. Bioanal. Chem.* **2017**. [CrossRef] [PubMed]
54. Berg, J.M.; Tymoczko, J.L.; Stryer, L. *Biochemistry*, 6th ed.; W. H. Freeman and Company: New York, NY, USA, 2007.
55. Zaidi, S.A.; Shin, J.H. Recent developments in nanostructure based electrochemical glucose sensors. *Talanta* **2016**, *149*, 30–42. [CrossRef] [PubMed]
56. Harrison, F.E.; May, J.M. Vitamin C Function in the Brain: Vital Role of the Ascorbate Transporter (SVCT2). *Free Radic. Biol. Med.* **2009**, *46*, 719–730. [CrossRef] [PubMed]
57. Meldrum, B.S. Glutamate as a neurotransmitter in the brain: Review of physiology and pathology. *J. Nutr.* **2000**, *130* (Suppl. 4S), 1007s–1015s. [PubMed]
58. Bruno, J.P.; Gash, C.; Martin, B.; Zmarowski, A.; Pomerleau, F.; Burmeister, J.; Huettl, P.; Gerhardt, G.A. Second-by-second measurement of acetylcholine release in prefrontal cortex. *Eur. J. Neurosci.* **2006**, *24*, 2749–2757. [CrossRef] [PubMed]
59. Gu, H.; Varner, E.L.; Groskreutz, S.R.; Michael, A.C.; Weber, S.G. In Vivo Monitoring of Dopamine by Microdialysis with 1 min Temporal Resolution Using Online Capillary Liquid Chromatography with Electrochemical Detection. *Anal. Chem.* **2015**, *87*, 6088–6094. [CrossRef] [PubMed]
60. Barros, L.F.; Deitmer, J.W. Glucose and lactate supply to the synapse. *Brain Res. Rev.* **2010**, *63*, 149–159. [CrossRef] [PubMed]
61. Mosharov, E.V.; Sulzer, D. Analysis of exocytotic events recorded by amperometry. *Nat. Methods* **2005**, *2*, 651–658. [CrossRef] [PubMed]